# The Etiology of Depression in Parkinson's Disease

Daphna Sourani[1], Renana Eitan[2] and Gadi Goelman[1]

[1]MRI/MRS Lab, the Human Biology Research Center
Department of Medical Biophysics
[2]Department of Psychiatry
Hadassah Hebrew University Medical Center,
Jerusalem, Israel

Corresponding author: Gadi Goelman, Ph.D.
MRI/MRS lab, the Human Biology Research Center
Department of Medical Biophysics
Hadassah Hebrew University Medical Center, Jerusalem, Israel
Tel: 972-2-6777769
Fax: 972-2-6421203
Email: gadig@hadassah.org.il

Keywords – Parkinson's disease, depression, unilateral 6-hydroxydopamine rat model, lateral habenula, dorsal Raphe, median Raphe, manganese-enhanced-MRI

## Abstract

Although a high percentage of Parkinson's disease (PD) patients suffer from depression in addition to their motor disabilities, the etiology of this depression is unknown. Within the framework of the monoamine deficiency hypothesis of depression, we present a neuronal circuitry that accounts for depression in PD. Using behavioral and direct neuronal circuitry measurements we show that the habenula mediates the coupling between the dopaminergic and the serotonergic systems and argue that alterations in basal ganglia activity cause habenula hyperactivity that result with depression in PD.

Behavioral results from novelty suppressed feeding and force swim tests, as well as direct circuitry measures with manganese enhanced MRI indicate (i) depressive-like behavior and reduced raphe nuclei connectivity/excitability in unilateral 6-hydroxydopamine injected rats, (ii) partial normalization of behavior and raphe connectivity after apomorphine treatment, and (iii) normalization of behavior after bilateral lesion of the habenula. These findings open up avenues for therapeutic intervention.

## Introduction

A high percentage of Parkinson's disease (PD) patients, who are known to undergo massive losses of dopamine neurons mainly within the substantia nigra pars compacta (SNc), suffer from depression and other disorders associated with a shortage of serotonin in addition to their motor disabilities. However, it is not clear whether these disorders are secondary to motor disabilities or whether there is a direct physiological link between PD and depression. Studies have shown evidence for coupling between the dopaminergic and the serotonergic systems but the mechanisms involved and the etiology of depression in PD remain unknown. There are reports on one hand, for example, of reduced dopamine levels[1,2] and increased D2 dopamine receptor-density in the basal ganglia (BG) and the cerebellum[3] in depressed patients. Serotonergic stimulation in the prefrontal cortex[4] or the striatum[5] on the other hand, has led to dopamine release. In addition, depressive-like behavior and reduced monoamine levels have been observed in 6-hydroxydopamine (6-OHDA) bilaterally injected rats[6-8], an animal model of PD.

Elsewhere we reported enhanced neuronal projections in unilateral 6-OHDA injected rats from BG output nuclei, particularly the globus palidus internal (GPi), to the lateral habenula (LHb) and from the LHb to the dorsal raphe nuclei (DRN) [9]. Drawing on these findings and viewing depression in PD as a neuronal circuitry disorder, we argue here that dysfunction of the dopaminergic system causes alterations in the serotonergic system that leads to depression. Specifically we claim that functional suppression of LHb activity uncouples these systems and can therefore improve behavior. We hypothesize that the enhanced LHb excitability in PD is the direct consequence of (*i*) the enhanced GPi activity known to occur in PD and (*ii*) the excitatory nature of the GPi→LHb projection[10,11]. Since the LHb→DRN projection is effectively inhibitory[12], it suggests a down-regulation of the serotonergic system in PD. We posit that this reduction is the major cause of reduced serotonin production in PD that leads to depression. LHb is thought to play a major role in major depression[13 14]. Anatomy tends to confirm this reasoning since the medial division of the LHb receives afferents primarily from limbic brain regions[15,16], whereas its lateral division is mainly innervated by the BG. Thus, LHb may be a convergence point for the limbic and BG circuits. Furthermore; LHb efferents primarily target nuclei containing monoamine neurons to control these systems[15-17], LHb was shown to play a critical role in negative reward[10,11,18], and hyperactivity of the LHb has been observed in depressed humans[19,20] and in certain animal models of depression[21,22].

To test this hypothesis we studied depression in a rat model of PD. We first report the behavioral validation of the appropriateness of our PD rat model (unilateral injection of 6-OHDA to the rat SNc) to study depression in PD. We then test our predictions for reduced raphe nuclei connectivity and activity in this model. Then we test the effect of dopamine replacement therapy on raphe nuclei excitability and connectivity and on behavior based on findings that L-DOPA[23,24] and dopamine agonists[25,26] reduce LHb activity whereas dopamine antagonists enhance it[27]. Finally we validate our hypothesis that functional suppression of LHb activity improves behavior. Two independent *in vivo* behavioral measures, the novelty suppressed feeding (NSF) test [28] which is a valid model for the stress-induced anxiety aspect of major depression [29] and the forced swim (FS) test [30] which is thought to model behavioral "despair" analogous to human depression[31] were used. To map spatiotemporal direct anterograde connectivity, manganese enhanced MRI (MEMRI)[32-34] with intracranial injection of manganese into the raphe nuclei was employed. This method detects manganese ion accumulation through its effect on the MRI signal. Manganese enters the neurons through voltage gated calcium channels, and then moves in an anterograde manner along axons and across synapses[35]. Since manganese accumulation is proportional to pathway efficiency and to pre-synaptic neuronal excitability, the strongest effective efferent pathways of the injection structure are revealed and excitability can be compared between groups.

## Results

Tyrosine Hydroxylase staining (for all MEMRI rats) or rate of rotations following aphomorphine injection (5mg/kg s.c), were used to control for the SNc lesion. 97.6± 1.12 % of the cells in the SNc of the left hemisphere were found to be destroyed in the stained rats and all others had higher than 8/min rotations in the contralateral direction of injection, thus meeting the criteria for the hemiparkinsonian rat model.

Feasibility of the animal model To demonstrate depression-like behavior, the NSF and FS tests were used (N=9/8 for the 'Sham' control group and N=13/12 for the unilateral 6-OHDA injected 'PD' rats, respectively). In the NSF test, food was removed for 36h prior to placing the rats in the corner of an open arena ($100\times100cm^2$) with food in its center. The times needed for first consumption the food (hereafter 'time') and the fractions of time the rats stayed in the periphery - an estimate of anxiety - ( hereafter 'thigmotaxis') were measured. Home cage consumption in the next half an hour and the average velocity in the first two minutes (V2) were measured to correct for unrelated effects. For the FS test, a pre-test for 15 min followed by a 5min test the next day were used. Rats were placed in a clear cylinder filled with water

(24±1$^0$C, 30 cm depth) and time of immobility (minimum movement to stay afloat), swimming, diving and climbing were measured by a blind observer (excluding the first 30s). Results of both tests are shown in Figure 1. As seen, both NSF measures and FS immobility time were significantly longer for the 'PD' rats (p=0.0013 and 0.009 for 'time' and ' thigmotaxis' on the NSF test, respectively using ANCOVA with V2 and food consumption as covariates, and p=0.001 one- tailed t-test for the FS test) demonstrating depression- like behavior. No velocity or food consumption effects were found between groups.

Raphe nuclei connectivity Based on the average rate of axonal manganese ion transport (2 mm/hour) [32], 96h were estimated to be sufficient for intra-neuronal manganese transportation from the raphe complex to regions of interest in the MEMRI measurements. Six T1-weighted MRI measurements were acquired for each animal at different times (baseline and at 3h, 24h, 48h, 72h and 96h post manganese injection). Figure 2 shows typical T1-weighted MRI images of the injection slice as a function of time from a manganese intra-cranial injection into the left Raphe interpositus (RIP) nucleus of a control rat. To minimize diffusion to the CSF and the bias it can cause, injections were targeted to the RIP assuming that sufficient manganese would extracellularly diffuse to the dorsal and median raphe nuclei. In general, manganese ions reduce water T1 values causing signal enhancements which are approximately proportional to manganese accumulation[36]. Extremely high manganese concentrations, as in the injection site 3h post injection, reduce T1 such that no signal is left. As can be seen in the figure, dark volumes match the left RIP. The injection sites, in all animals, were located within the left RIP. By extra-cellular diffusion, the volume of enhanced signal increased approximately symmetrically with time and its signal decreased towards baseline. Figure 3 shows three series of T1-weighted images taken from the same slice that was approximately 6mm from the injection site (-3.8 from Bregma). These images were obtained by averaging the images from all sham (3a), all 6-OHDA injected rats (3b) and all 6-OHDA rats treated with apomorphine (3c). This figure shows averaging to illustrate the consistency across individual animals and facilitate visualization of the enhanced signal. In this slice, significant signal enhancements were observed in all rats in the habenula (mainly LHb), the hippocampus (the dentate gyrus), the thalamus and the hypothalamus of both hemispheres. Signal intensity in these structures increased at 3h and 24h, and remained strong for the entire times measured. Note that this pattern is completely different from the one observed at the injection site (Figure 2, insert), thus illustrating two independent processes that are hypothesized to be extra-cellular diffusion (Figure 2) and intra-cellular propagation

(Figure 3). Enhancements in other slices were either too weak or not common to most of the animals. Selecting regions of interest (ROIs) for quantitative analysis from these images was difficult. While ROIs for the habenula could be selected based on anatomy, in the hippocampus, hypothalamus and the thalamus this was quite complex since signal intensity in these areas was enhanced only in specific loci and with different volumes at different time points. For these reasons, a spatiotemporal factor-analysis method was used on the sham injected rat data and its results, six selected ROIs, was applied to all rats (see method). Three functional ROIs for each hemisphere were defined (Figure 1B&C, supplementary data): the LHb, volume within the dentate gyrus of the hippocampus, and the volume within the hypothalamic nuclei. ANOVAs with repeated measures revealed significant higher signal enhancements in the sham group: $F(1,12)=63.75$, $p<0.0001$, and significant difference between time points: $F(5,90)=20.57$, $p<0.0001$. Furthermore, a significant time*group interaction effect was found: $F(5,90)=17.08$, $p<0.0001$. No significant ROI effect was observed although at time=72h, the enhancement in the thalamus was different than in the hippocampus. These results demonstrate reduced connectivity and excitability of the raphe in 6-OHDA injected rats (Figure 5).

Effect of treatment with apomorphine Apomorphine, a dopamine replacement therapy, was shown to reduce glucose utilization in the LHb [26] and thus, in line with our hypothesis, should improve behavior and raphe connectivity/excitability. To test this prediction, daily injections of apomorphine (10mg/Kg s.c.), were used and (*i*) raphe nuclei connectivity/excitability was measured by MEMRI (N=7) and (*ii*) depressed like behavior was measured by the NSF and FS tests (N=12 for 6-OHDA+apomorphine, marked as 'PD+Apo'). Figure 4 shows the behavioral, and Figures 3&5 the MEMRI results. Whereas apomorphine normalized behavior in the NSF test ($p=0.0004$ and $0.0059$ for 'time' and ' thigmotaxis', respectively), it did not show a significant effect on the FS test ($p=0.135$). ANOVAs with repeated measures for the MEMRI data revealed significant differences between the 'PD' and the 'PD+Apo' groups: $F(1,12)=13.24$, $p=0.0005$, and between time points: $F(5,90)=16.47$, $p<0.0001$. No significant ROI effect was observed although at time=48h, the enhancement in the thalamus was different than in the hippocampus and at time=72h the habenula was higher than the hippocampus. For completeness, we calculated the differences between the MEMRI enhancements of the 'Sham' and the 'PD+Apo' groups. A significant group effect was found, $F(1,12)=29.55$, $p<0.0001$ as well as a time effect, $F(5,90)=23.43$ $p<0.0001$ and time*group interaction effect, $F(5,90)=6.37$, $p<0.0001$. Figure 5 shows the combined signal enhancements from all ROI for 'Sham', 'PD' and 'PD+Apo'. As

seen, at all time points (beside baseline) signal enhancements of the 'PD+Apo' rats was between the signal of the 'PD' and the 'Sham' rats, thus demonstrating a positive (although partial) effect of apomorphine treatment.

Effect of habenula lesion The final test was to measure the result of functional suppression of LHb activity. Bilateral electric lesions (1mA for 15 seconds[37]) of the habenula were used and their locations verified by MRI. Lesions were found to cover the entire habenula complex and therefore prevented reliable evaluation of enhancements in the MEMRI experiments. Two weeks after electrical lesion, the NSF and FS tests were performed (N=8 for the 'Sham+lesion' and N=9 for the 'PD+lesion'). In all tests, the control rats with and without habenula lesion were not distinguishable (p=0.813 and 0.612 for the 'time' and 'thigmotaxis' of the NSF, respectively and p=0.489 for the FS tests) suggesting that behavioral impairments of the lesion itself were not present on these tests. Figure 6 shows the positive effect of habenula lesion for both tests which is congruent with our hypothesis: for the 'time' parameter (left diagram), no difference between habenula lesion groups was observed (p=0.95) and 'PD+lesion' rats had a significantly lower 'time' than 'PD' rats (p=0.006). For the 'thigmotaxis' parameter (center diagram), no difference between habenula lesion groups was observed (p=0.27) and 'PD+lesion' rats showed a tendency for smaller 'thigmotaxis' (p=0.076). For the FS test (right diagram), the habenula lesion groups were undistinguishable (p=0.498) whereas 'PD+lesion' rats had shorter immobility times compared with 'PD' rats (p=0.004).

## Discussion

Based on the postulate that the prime effect in PD is dopamine cell death primarily in the SNc, our 6-OHDA injection rat model was used to study the etiology of depression in PD. Our current and previous[9] results on 6-OHDA injected rats suggest sequential events that start with dopamine cell loss, continue with enhanced LHb activity, then cause reduced raphe excitability which, in line with the monoamine deficiency hypothesis, lead to depression. Due to the feedback connections between these structures, we hypothesize that depression is likely to develop regardless of where the initial failure occurs. Consequently, depression in PD shares features with general depression such that understanding its etiology will further our knowledge of the etiology of general depression as well.

The depressive-like behavior of the unilateral 6-OHDA injected rats, as was verified by the NSF and the FS tests, confirmed the relevance of the model. Although assessment of mood-related behaviors in animals is complex with multiple interpretations[38,39], the abnormality

demonstrated by the NSF and FS tests is sufficient to presume some "depressive-like" behavior and therefore supports the validity of the model to study the etiology of depression in PD.

To test whether this depressive-like behavior was the outcome of reduced serotonergic activity, we conducted MEMRI of the raphe nuclei. Generally, intracranial manganese ion injection generates two modes of transfer. Extracellular ion diffusion, characterized by radial symmetry, proximity to the injected site, and a decreasing manganese concentration along time. The second mode, intracellular anterograde propagation, is characterized by distinct and well-localized clusters of signal enhancement whose strength is proportional to the amount of manganese accumulation. Manganese accumulation depends on the excitability of the pre-synaptic neuron(s) through the excitability of L-type calcium channels[40-44], the length of the projection pathway [45,46] and synaptic efficacy. Signal enhancements were observed around the injection site (Figure 2) and at several clusters located about 6mm away (Figure 3). However, the spatiotemporal patterns of these signal enhancements were very different. The signal enhancement around the injection site exhibited approximate spherical symmetry whose maximum occurred immediately after manganese injection. Signal intensity faded away with time and its radius increased. In contrast, highly localized signal enhancements with defined borders were observed ~6mm from the injection site in various locations whose enhancements increased to a maximum at 24h and then reduced (Figure 1A, supplementary). These temporal patterns suggest two different processes; namely, extracellular diffusion for the former and intracellular propagation for the latter. Given these features, we assume that signal enhancements in the slice shown in Figure 3 correspond to neuronal propagation from the raphe, particularly from the dorsal and median raphe. The obtained ROIs are in line with known efferents of the raphe nuclei[12,47,48] with other efferents either weaker or ones whose targets are highly interconnected causing manganese to spread fast, thus difficult to observe (e.g. cortex). Since there was no ROI effect in the analysis, no specific raphe efferent could be identified as affected by BG abnormality. Consequently, the lower signal enhancement in the 6-OHDA rat group was interpreted as a homogeneous reduction of raphe excitability, thus supporting our hypothesis for a down-regulation of the raphe nuclei by dopamine deficiency. The depressed-like behavior of this group was therefore in line with the monoamine deficiency (reduced serotonin production) and the hippocampal neurogenesis (the altered raphe- dentate gyrus connection) hypotheses of depression.

Since apomorphine treatment increases dopamine availability and reduces habenula activity[26], we tested its effects on behavior and on raphe connectivity. Whereas the NSF test

demonstrated normalization by apomorphine treatment, the FS test failed to show such an effect (Figure 4). Similarly, MEMRI demonstrated a positive effect of apomorphine which resulted in partial normalization of raphe connectivity as seen in Figures 3&5. At all time points, apomorphine treated rats showed higher enhancements compared with 'PD' rats but lower enhancements than 'Sham' rats. These and the behivour results support our hypothesis of the critical role of the habenula in modulating raphe excitability and thus behivior.

Finally we tested whether behavior can be improved by functional suppression of habenula activity. An electrical lesion rather than high frequency stimulation was used due to its ease and global effect. Due to the simplicity of our circuitry model, we cannot predict the exact effect of LHb lesion on behavior. Consequently, full or partial behavioral normalization suggests general agreement with the model. Our findings of normalization on the NSF test (although only a trend was observed on the anxiety measure) and the FS test are therefore congruent with the model. This suggests that functional suppression of the habenula results in improved behavioral response, in line with recent reports on a human depressed patient[14].

In summary, the qualitative agreement between the MEMRI and the behavioral measurements for the 6-OHDA rats and the 6-OHDA rats with apomorphine treatment, although each provided information on a different scale, suggest a direct link between dopamine deficiency, serotonin activity and depressed-like behavior. Moreover, our data support the claim that the habenula mediates this linkage. Thus SNc cell destruction is likely to cause GPi and LHb hyperactivity, which in turn down-regulates dorsal and median raphe excitability, hence leading to depression. Dopamine replacement therapy and habenula lesion partially reverse these processes, resulting in improved behavior and enhanced raphe connectivity. Although the beneficial effects of dopamine on depression are not new[49], these findings suggest a possible mechanism for its effect. Our results may provide a physiological explanation for the clinical observation of the high percentage of depressed PD patients, and open up new avenues for therapeutic approaches, for example deep brain stimulation, to assist these patients.

Acknowledgments We thank Dr. Lucas Lecourtier for providing relevant references and Mr. Chaim Karger and Dr. Tarrasch for the statistical analysis. This work was supported by the Israel Science Foundation grants no. 184/05 and 1334/08.

## Figure Captions

1.Average parameters ± their standard error from the novelty suppressed feeding (NSF) and the forced swim (FS) tests. Sham injected controls (marked 'Sham') were compared to unilateral 6-OHDA injected to the SNc rats (marked 'PD'). ANCOVA indicated a significantly lower 'time to reach the center', a measure of depression (left diagram), and a significantly longer time in the periphery, a measure of anxiety (middle diagram), in the 'PD' group. A T-test for the immobility time in the FS test (right diagram) showed a significant difference between the groups, with longer times for the 'PD' group. These results indicate that the unilateral 6-OHDA injected rats show depression- like behavior and therefore are a good model to study depression in PD.

2.A typical example of MEMRI data of a sham injected rat in the injection slice. T1-weighted images taken before, at 3h, 24h, 48h, 72h and 96h post manganese injection. Manganese ions were injected into the Raphe interpositus nucleus. The dark area in the middle of the bright volume marks the injection site (the lowest T1 values) whereas the moderate decrease in T1 in the surrounding areas results in the bright signal. Signal enhancement fades with time and its radius increases, as is typical for an extra-cellular diffusion process. The temporal pattern of the ROI marked by a dashed line is inserted. For anatomical identification, the rat brain atlas of that slice is overlaid on the baseline image.

3.Average images of the sham injected rats (**a**), the 6-OHDA injected rats (**b**) and the 6-OHDA injected rats treated with apomorphine (**c**), at 4 (out of 6) time points obtained by the manganese enhanced MRI method after intracranial manganese injection into the raphe nuclei complex. Signal enhancements are seen in the dentate gyrus of the hippocampus, the habenula complex (mainly the LHb), the thalamic and the hypothalamic areas of both hemispheres. As seen, enhancements differ in intensity and temporal pattern between the groups, with stronger signal enhancements in the sham injected rats which suggests reduced efferent connectivity of the raphe nuclei in the 6-OHDA injected rats. For anatomical identification, the rat brain atlas of that slice is overlaid on the baseline image of the sham group.

4. Average parameters ± their standard error from the novelty suppressed feeding (NSF) and the forced swim (FS) tests for the comparison between 6-OHDA injected rats with (marked 'PD+Apo') and without (marked 'PD') apomorphine treatment (daily injection of 10mg/kg). 'Time to reach the center', (left diagram), and time in the periphery, (middle diagram) are significantly normalized. However, immobility time in the FS test (right diagram) showed

no significant difference between the groups. These results demonstrate a partial effect of apomorphine treatment on behavior.

5. Average from all ROIs ± its standard error of the normalized MRI signal intensity along time from manganese injection for the 'Sham', unilateral 6-OHDA injected ('PD') and unilateral 6-OHDA injected + apomorphine treatment ('PD+Apo') groups. Significantly lower signal enhancements of the 'PD' rats compared with the 'Sham' rats are seen. Apomorphine treatment resulted in higher signal enhancement compared with 'PD' rats but lower compared with the 'Sham' rats. It demonstrates reduced raphe excitability of the 6-OHDA rats with partial normalization by apomorphine treatment.
6. Average parameters ± their standard error from the novelty suppressed feeding (NSF) and the forced swim (FS) tests for the comparison between sham injected rats with bilateral lesion of the habenula (marked 'Sham+lesion') and 6-OHDA injected rats with bilateral lesion of the habenula (marked 'PD+lesion'). For easy visualization, the control without habenula lesion ('Sham') and the 6-OHDA injected rats ('PD') in Figure 1 are also shown. Two main effects of habenula lesion are seen. One is that the 'Sham' and the 'Sham+lesion' groups were indistinguishable, and the other is the positive effect of the lesion on the 'PD' rats. In all tests, no differences between groups with habenula lesion were observed. More importantly, the habenula lesion seemed to normalize the behavior of 'PD' rats in all tests (see text) indicating general agreement with our hypothesis.

Supplemental figure

1. Model-free spatiotemporal factor analysis for the definition of functional-ROIs. **A**. The high variance (43.1%) temporal function obtained from all the sham injected rats together. It depicts signal enhancement whose maximum is at 24h post manganese injection. **B**. Coincident map of a slice -3.8mm from the bregma showing a color coded overlap between function-maps of individual sham injected rats. Each functional-map presents those pixels whose weight of the function in A is significant. Color represents the amount of overlap of these pixels between rats in percentages. **C**. The six functional-ROI: the LHb, within the hippocampus, and within the hypothalamus. These ROIs were defined as the volumes whose overlap between individual functional-maps is above 43% of the sham injected rats as guided by the coincident map of **B**.

## Materials and Method

Animals and surgery The surgery and procedures were approved by the *Animal Care and Use Committee of the Hebrew University*. Five male Sprague-Dawley (250-400g) rat groups were used: Saline (termed 'Sham') and 6-hydroxydopamine (termed 'PD') injection to the left substantia nigra part compacta (SNc); 'PD' rats with 10mg/Kg apomorphine (injected s.c. every 24h, termed 'PD+Apo'); 'Sham' rats with sham bilateral habenula lesions (termed 'Sham+lesion') and 'PD' rats with bilateral habenula lesion (termed 'PD+lesion'). MEMRI performed 14d after SNc surgery, the NSF/FS tests at 14/17-18 after SNc surgery, and behavioral tests for the last two groups, at 17-18d post electric lesion that was 14d after SNc surgery.

Rats were anesthetized with ketamine (90 mg/kg i.p. Sigma, Israel) plus xylazine (5mg/kg i.p. Sigma, Israel) and rimadyl was administered for 3 days following surgery. Body weight and general behavior were monitored for several days post surgery. For the 6-OHDA/Saline injection, rats were stereotaxically injected (1μL/min) into the left SNc (AP: -0.48, ML: 0.16, DV: -0.84) with either 4 μl of 10mM 6-OHDA hydrochloride with 0.01% ascorbic acid (Sigma, Israel) or with saline solution (0.9%). For the MEMRI experiments, rats were injected (0.1 μl/min) with $MnCl_2$, (0.4μL; 0.08M) into the left Raphe interpositus nucleus (AP:-0.93, ML:0.03,DV:-0.8). For the electrical LHb lesion, 1mA current for 10s was applied through two electrodes (one at a time) inserted into the right and left habenula (AP:-0.39 ML:+/- 0.1 DV:-0.47).

Histology

All 'PD' rats that underwent MEMRI were perfused, sliced and Tyrosine Hydroxylase-immunohistochemistry of the SNc performed (Patho-Lab Diagnostic Nes Ziona, Israel). Cells were manually counted in each animal and hemisphere.

NSF test

After 36h without food, rats were placed in a corner of an open-field arena ($1\times1m^2$ with 4cm high edges) containing 10 pellets of food in its center. The time before first food consumption ('time'), and the time in the periphery (' thigmotaxis' - defined as the 20cm wide square along the edges), were measured. The velocity in the first 2min and total home cage consumption (30min after the test) were used as covariates. Maximum experimental time was set to 10min.

FS test

Rats were placed in a clear cylinder filled with water ($24\pm1^0$c, 30cm depth) and their motion recorded. Time of immobility (minimal movement to stay afloat), swimming, diving and

climbing were measured. Immobility was used for comparison. A pre-test for 15 min with the main test a day later were performed[50,51].

MRI

Six MEMRI sessions, (before, 3h, 24h, 48h, 72h and 96h post manganese injection) were conducted using a 4.7 T Bruker BioSpec scanner (Bruker Biospin Ettlington, Germany). Rats were anesthetized with isoflurane (2% + 30:70 $O_2$:$N_2O$) and respiration rate (0.75-1 Hz) and body temperature (37$^{o}$C ±1), were kept stable. 2D T1-weighted coronal gradient-echo images (TR=58ms, TE=3.1ms, flip angle 15$^{o}$, matrix=256×192, zero filled to 256×256, 1mm slices, FOV=3×3cm and 100 averages), were acquired.

MRI Data Analysis

Custom software in IDL (Interactive Data Language, version 6.1, USA) and commercial factor analysis software (Pixies standard edition 1.11, France) were used. Images were realigned, within and between rats, the rat brain atlas[52] wrapped over, and images were normalized by the baseline images. Factor analysis was restricted to positive pixels and to three positive functions. It was applied on the sham rat group. On each sham rat separately, it revealed one common high variance function (39.5%±2.9), and on all sham rats, one high-variance function (43.1%, Figure 1A , supplementary data) that was similar to the common functions of the individual rat analysis. The other two functions (in both analyses) were high frequency fluctuations whose spatial coverage scattered in the entire slice. ROIs were defined using the spatial coverage of the high variance function as follows: (i) The distribution of this function's weights was calculated for each animal separately and was fitted to a Gaussian. Cutoffs were defined as the Gaussian mean+1.2SD. (ii) The pixels above cutoff defined function-maps for each rat. (iii) A group coincidence map was obtained by spatial overlap between function-maps (figure 1B in the supplementary data). (iv) Functional-ROIs were pixels that coincided in >42% of the sham rats within the following structures: the LHb, within the hippocampus and within the hypothalamus of both hemispheres (figure 1C, supplementary data).

Statistics

Analysis of covariance (SAS, 8.0) with rat-group as the independent variable and V2 and food consumption as covariates was used for the NSF test. Statistics were obtained for the 'time' and 'thigmotaxis' parameters separately. A one- tailed t-test was used for the FS test. ANOVA with repeated measures (2(groups) x 3 (ROI) x (6 time)) was used for the MEMRI

data after averaging ROIs from the two hemispheres since no hemispheric effect was found. Significance was set at $p=0.05$.

## References


1. Lambert, G., Johansson, M., Agren, H. & Friberg, P. Reduced brain norepinephrine and dopamine release in treatment-refractory depressive illness: evidence in support of the catecholamine hypothesis of mood disorders. *Arch Gen Psychiatry* **57**, 787-793 (2000).
2. McLean, A., Rubinsztein, J.S., Robbins, T.W. & Sahakian, B.J. The effects of tyrosine depletion in normal healthy volunteers: implications for unipolar depression. *Psychopharmacology (Berl)* **171**, 286-297 (2004).
3. D'Haenen H, A. & Bossuyt, A. Dopamine D2 receptors in depression measured with single photon emission computed tomography. *Biol Psychiatry* **35**, 128-132 (1994).
4. Chen, J., Paredes, W., Van Praag, H.M., Lowinson, J.H. & Gardner, E.L. Presynaptic dopamine release is enhanced by 5-HT3 receptor activation in medial prefrontal cortex of freely moving rats. *Synapse* **10**, 264-266 (1992).
5. El Yacoubi, M., Costentin, J. & Vaugeois, J.M. Adenosine A2A receptors and depression. *Neurology* **61**, S82-87 (2003).
6. Tadaiesky, M.T.*, et al.* Emotional, cognitive and neurochemical alterations in a premotor stage model of Parkinson's disease. *Neuroscience* **156**, 830-840 (2008).
7. Branchi, I.*, et al.* Nonmotor symptoms in Parkinson's disease: investigating early-phase onset of behavioral dysfunction in the 6-hydroxydopamine-lesioned rat model. *J Neurosci Res* **86**, 2050-2061 (2008).
8. Zhang, X., Andren, P.E. & Svenningsson, P. Changes on 5-HT2 receptor mRNAs in striatum and subthalamic nucleus in Parkinson's disease model. *Physiol Behav* **92**, 29-33 (2007).
9. Pelled, G., Bergman, H., Ben-Hur, T. & Goelman, G. Manganese-enhanced MRI in a rat model of Parkinson's disease. *J Magn Reson Imaging* **26**, 863-870 (2007).
10. Matsumoto, M. & Hikosaka, O. Lateral habenula as a source of negative reward signals in dopamine neurons. *Nature* **447**, 1111-1115 (2007).
11. Matsumoto, M. & Hikosaka, O. Representation of negative motivational value in the primate lateral habenula. *Nature neuroscience* **12**, 77-84 (2009).
12. Ferraro, G., Montalbano, M.E., Sardo, P. & La Grutta, V. Lateral habenula and hippocampus: a complex interaction raphe cells-mediated. *J Neural Transm* **104**, 615-631 (1997).
13. Sartorius, A. & Henn, F.A. Deep brain stimulation of the lateral habenula in treatment resistant major depression. *Med Hypotheses* **69**, 1305-1308 (2007).
14. Sartorius, A.*, et al.* Remission of major depression under deep brain stimulation of the lateral habenula in a therapy-refractory patient. *Biological psychiatry* **67**, e9-e11.
15. Herkenham, M. & Nauta, W.J. Afferent connections of the habenular nuclei in the rat. A horseradish peroxidase study, with a note on the fiber-of-passage problem. *J Comp Neurol* **173**, 123-146 (1977).
16. Geisler, S. & Trimble, M. The lateral habenula: no longer neglected. *CNS spectrums* **13**, 484-489 (2008).
17. Araki, M., McGeer, P.L. & Kimura, H. The efferent projections of the rat lateral habenular nucleus revealed by the PHA-L anterograde tracing method. *Brain Res* **441**, 319-330 (1988).
18. Hikosaka, O., Sesack, S.R., Lecourtier, L. & Shepard, P.D. Habenula: crossroad between the basal ganglia and the limbic system. *J Neurosci* **28**, 11825-11829 (2008).
19. Morris, J.S., Smith, K.A., Cowen, P.J., Friston, K.J. & Dolan, R.J. Covariation of activity in habenula and dorsal raphe nuclei following tryptophan depletion. *Neuroimage* **10**, 163-172 (1999).

20. Smith, K.A., Morris, J.S., Friston, K.J., Cowen, P.J. & Dolan, R.J. Brain mechanisms associated with depressive relapse and associated cognitive impairment following acute tryptophan depletion. *Br J Psychiatry* **174**, 525-529 (1999).
21. Caldecott-Hazard, S., Mazziotta, J. & Phelps, M. Cerebral correlates of depressed behavior in rats, visualized using 14C-2-deoxyglucose autoradiography. *J Neurosci* **8**, 1951-1961 (1988).
22. Shumake, J., Edwards, E. & Gonzalez-Lima, F. Opposite metabolic changes in the habenula and ventral tegmental area of a genetic model of helpless behavior. *Brain Res* **963**, 274-281 (2003).
23. Trugman, J.M. & Wooten, G.F. The effects of L-DOPA on regional cerebral glucose utilization in rats with unilateral lesions of the substantia nigra. *Brain Res* **379**, 264-274 (1986).
24. Trugman, J.M., Hubbard, C.A. & Bennett, J.P., Jr. Dose-related effects of continuous levodopa infusion in rats with unilateral lesions of the substantia nigra. *Brain Res* **725**, 177-183 (1996).
25. Porrino, L.J., Lucignani, G., Dow-Edwards, D. & Sokoloff, L. Correlation of dose-dependent effects of acute amphetamine administration on behavior and local cerebral metabolism in rats. *Brain Res* **307**, 311-320 (1984).
26. McCulloch, J., Savaki, H.E. & Sokoloff, L. Influence of dopaminergic systems on the lateral habenular nucleus of the rat. *Brain Res* **194**, 117-124 (1980).
27. Trugman, J.M. & James, C.L. D1 dopamine agonist and antagonist effects on regional cerebral glucose utilization in rats with intact dopaminergic innervation. *Brain Res* **607**, 270-274 (1993).
28. Bodnoff, S.R., Suranyi-Cadotte, B., Aitken, D.H., Quirion, R. & Meaney, M.J. The effects of chronic antidepressant treatment in an animal model of anxiety. *Psychopharmacology (Berl)* **95**, 298-302 (1988).
29. Dulawa, S.C. & Hen, R. Recent advances in animal models of chronic antidepressant effects: the novelty-induced hypophagia test. *Neurosci Biobehav Rev* **29**, 771-783 (2005).
30. Detke, M.J., Rickels, M. & Lucki, I. Active behaviors in the rat forced swimming test differentially produced by serotonergic and noradrenergic antidepressants. *Psychopharmacology (Berl)* **121**, 66-72 (1995).
31. Borsini, F. & Meli, A. Is the forced swimming test a suitable model for revealing antidepressant activity? *Psychopharmacology (Berl)* **94**, 147-160 (1988).
32. Pautler, R.G., Silva, A.C. & Koretsky, A.P. In vivo neuronal tract tracing using manganese-enhanced magnetic resonance imaging. *Magn Reson Med* **40**, 740-748 (1998).
33. Koretsky, A.P. & Silva, A.C. Manganese-enhanced magnetic resonance imaging (MEMRI). *NMR Biomed,* **17**, 529-539 (2004).
34. Saleem, K.S.*, et al.* Magnetic resonance imaging of neuronal connections in the macaque monkey. *Neuron* **34**, 685-700 (2002).
35. Pautler, R.G., Silva, A.C. & Koretsky, A.P. In vivo neuronal tract tracing using manganese-enhanced magnetic resonance imaging. *Magn Reson Med* **40**, 740 (1998).
36. Silva, A.C. & Bock, N.A. Manganese-Enhanced MRI: An Exceptional Tool in Translational Neuroimaging. *Schizophr Bull* (2008).
37. Thornton, E.W. & Bradbury, G.E. Effort and stress influence the effect of lesion of the habenula complex in one-way active avoidance learning. *Physiol Behav* **45**, 929-935 (1989).
38. Cryan, J.F. & Holmes, A. The ascent of mouse: advances in modelling human depression and anxiety. *Nature reviews* **4**, 775-790 (2005).

39. Ramos, A., Pereira, E., Martins, G.C., Wehrmeister, T.D. & Izidio, G.S. Integrating the open field, elevated plus maze and light/dark box to assess different types of emotional behaviors in one single trial. *Behavioural brain research* **193**, 277-288 (2008).
40. Merritt, J.E., Jacob, R. & Hallam, T.J. Use of manganese to discriminate between calcium influx and mobilization from internal stores in stimulated human neutrophils. *J Biol Chem* **264**, 1522-1527 (1989).
41. Simpson, P.B., Challiss, R.A. & Nahorski, S.R. Divalent cation entry in cultured rat cerebellar granule cells measured using Mn2+ quench of fura 2 fluorescence. *Eur J Neurosci* **7**, 831-840 (1995).
42. Wiemann, M., Busselberg, D., Schirrmacher, K. & Bingmann, D. A calcium release activated calcium influx in primary cultures of rat osteoblast-like cells. *Calcif Tissue Int* **63**, 154-159 (1998).
43. Du, C., MacGowan, G.A., Farkas, D.L. & Koretsky, A.P. Calibration of the calcium dissociation constant of Rhod(2)in the perfused mouse heart using manganese quenching. *Cell Calcium* **29**, 217-227 (2001).
44. Tisch-Idelson, D., Sharabani, M., Kloog, Y. & Aviram, I. Stimulation of neutrophils by prenylcysteine analogs: Ca(2+) release and influx. *Biochim Biophys Acta* **1451**, 187-195 (1999).
45. Revital, S., Hagai, B. & Gadi, G. Evidence for the coexistence of segregated and integrated functional connections from the striatum to the substantia nigra in rats. *NeuroImage* **40**, 451-457 (2008).
46. Doron, O. & Goelman, G. Evidence for asymmetric intra substantia nigra functional connectivity-application to basal ganglia processing. *NeuroImage* (2009).
47. Segal, M. The action of serotonin in the rat hippocampal slice preparation. *The Journal of physiology* **303**, 423-439 (1980).
48. Conrad, L.C., Leonard, C.M. & Pfaff, D.W. Connections of the median and dorsal raphe nuclei in the rat: an autoradiographic and degeneration study. *The Journal of comparative neurology* **156**, 179-205 (1974).
49. Clausius, N., Born, C. & Grunze, H. [The relevance of dopamine agonists in the treatment of depression.]. *Neuropsychiatr* **23**, 15-25 (2009).
50. Haidkind, R.*, et al.* Effects of partial locus coeruleus denervation and chronic mild stress on behaviour and monoamine neurochemistry in the rat. *Eur Neuropsychopharmacol* **13**, 19-28 (2003).
51. Banasr, M. & Duman, R.S. Glial loss in the prefrontal cortex is sufficient to induce depressive-like behaviors. *Biological psychiatry* **64**, 863-870 (2008).
52. Paxinos, G. & Watson, C. *The Rat Brain in Stereotactic Coordinates*, (Academic Press, 1997).

Figure 1

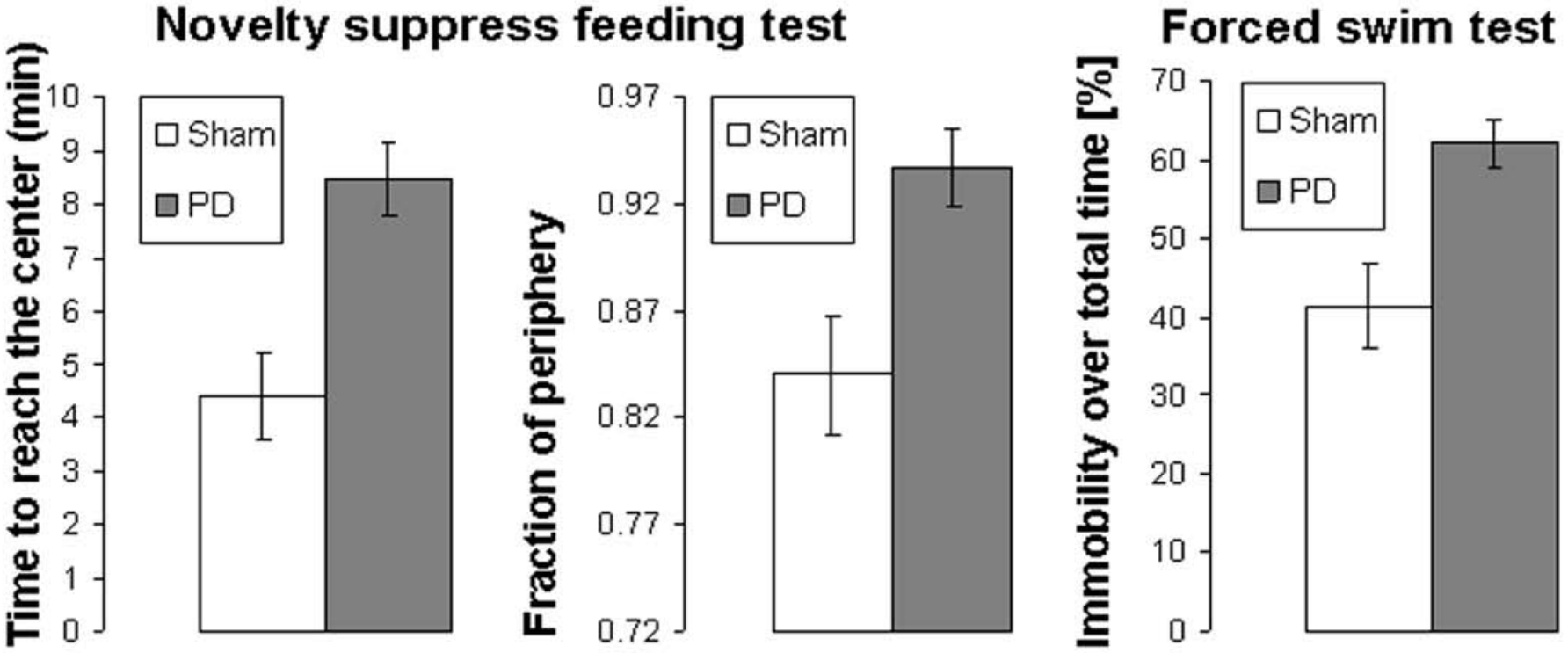
Novelty suppress feeding test
Time to reach the center (min)
0
1
2
3
4
5
6
7
8
9
10
Sham
PD
Fraction of periphery
0.72
0.77
0.82
0.87
0.92
0.97
Sham
PD
Forced swim test
Immobility over total time [%]
0
10
20
30
40
50
60
70
Sham
PD

# Figure 2

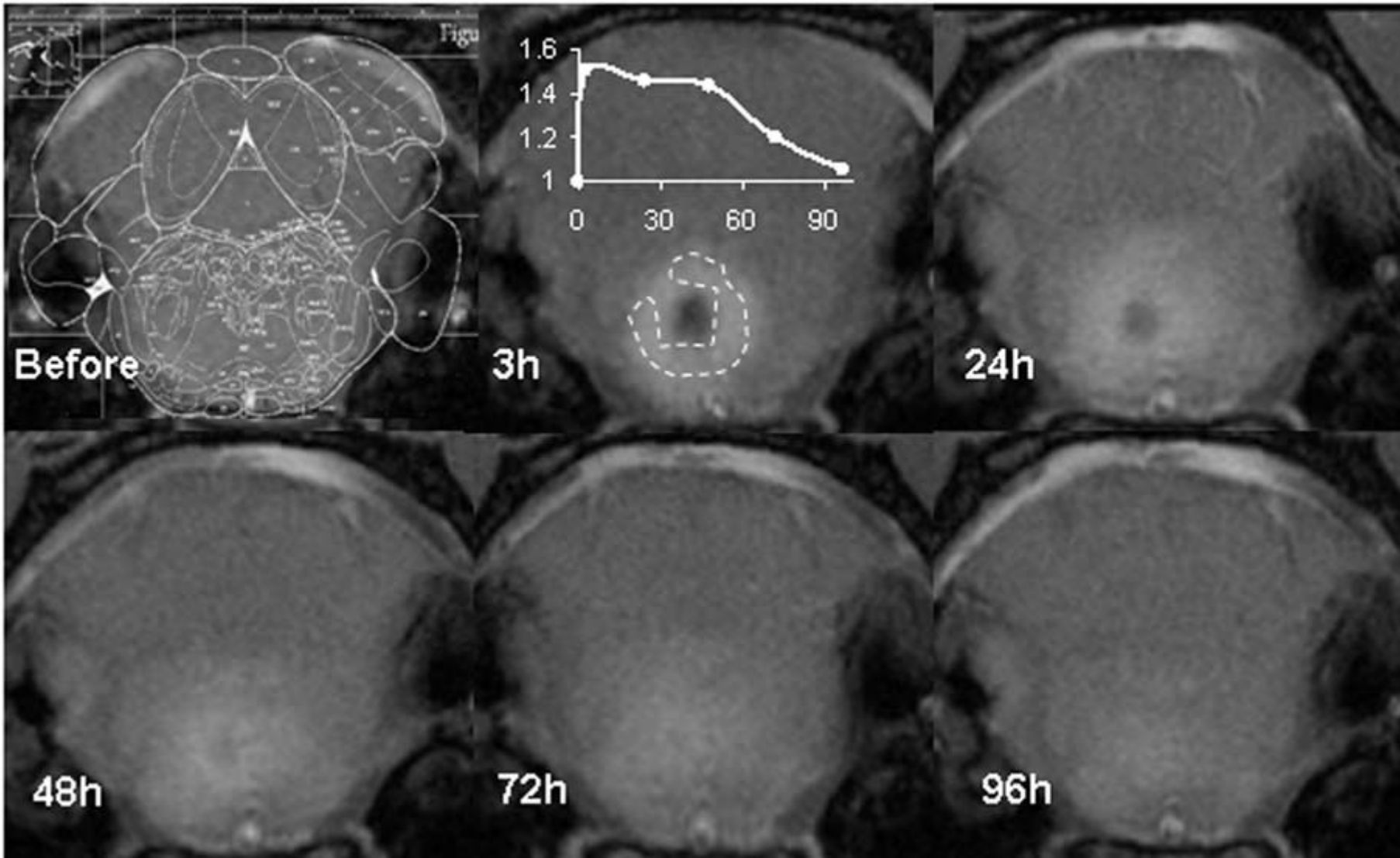

# Figure 3

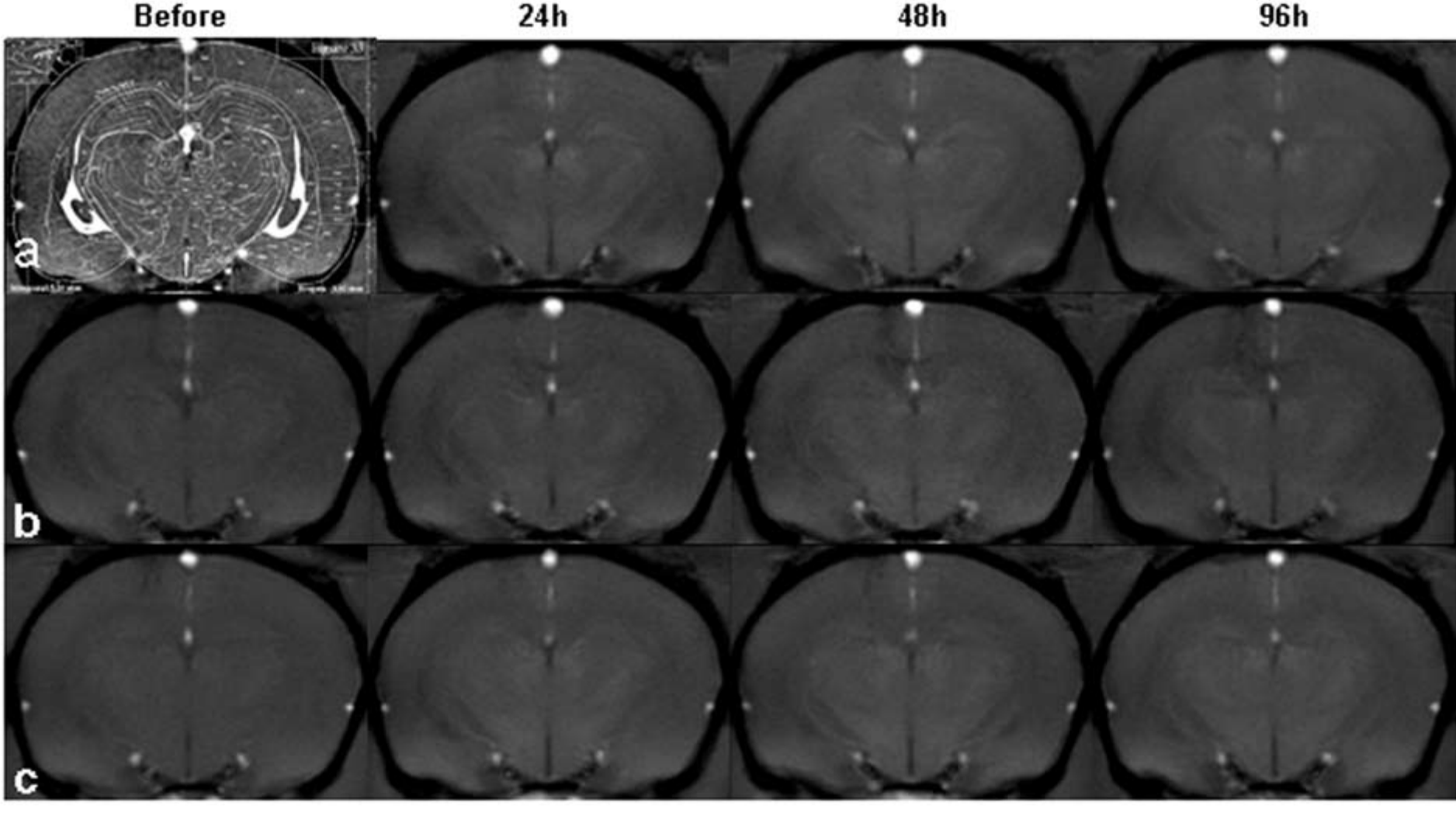

Figure 4

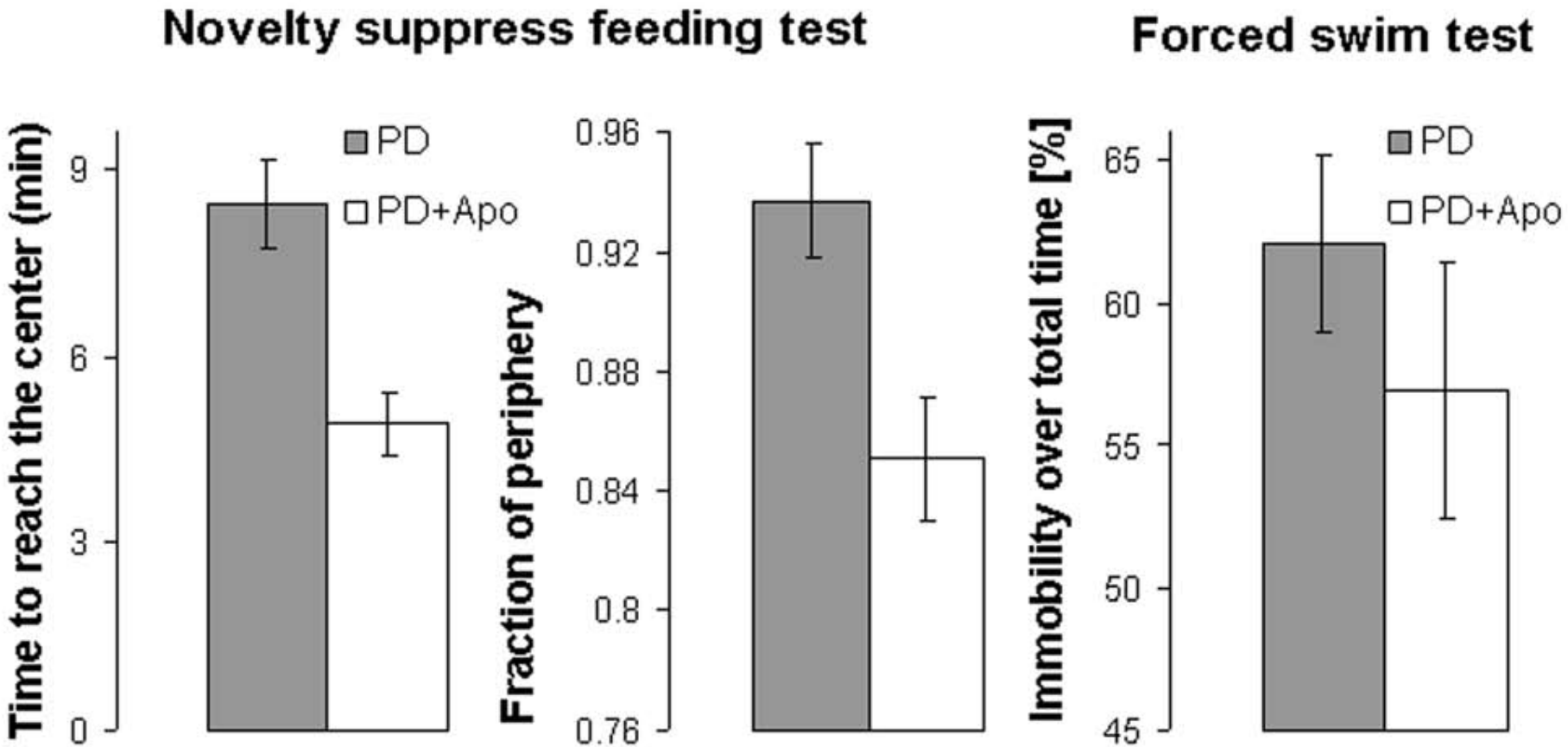
Novelty suppress feeding test
Time to reach the center (min)
9
6
3
0
PD
PD+Apo
Fraction of periphery
0.96
0.92
0.88
0.84
0.8
0.76
Forced swim test
Immobility over total time [%]
65
60
55
50
45
PD
PD+Apo

# Figure 5

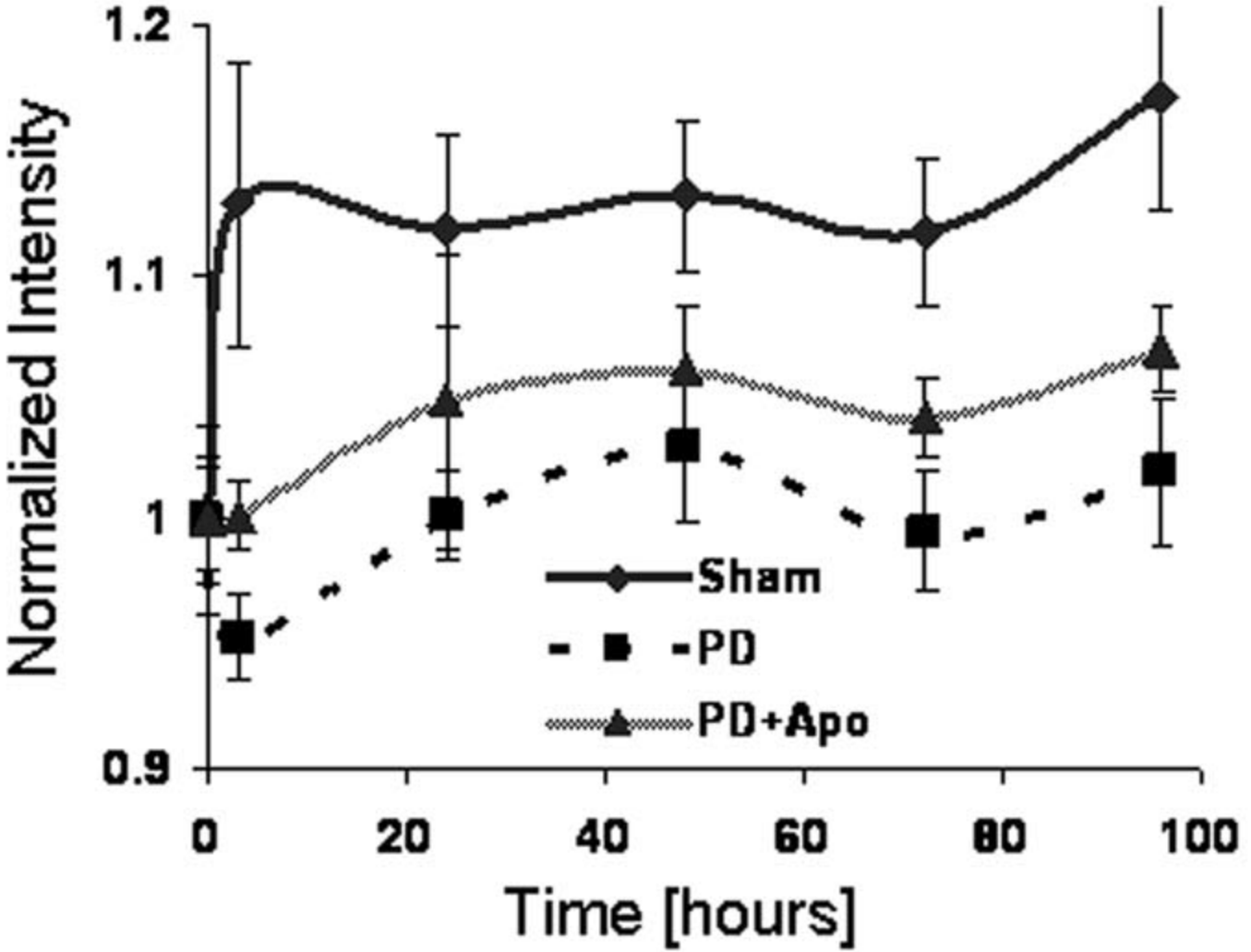
1.2
1.1
1
0.9
Normalized Intensity
0
20
40
60
80
100
Time [hours]
Sham
PD
PD+Apo

Figure 6

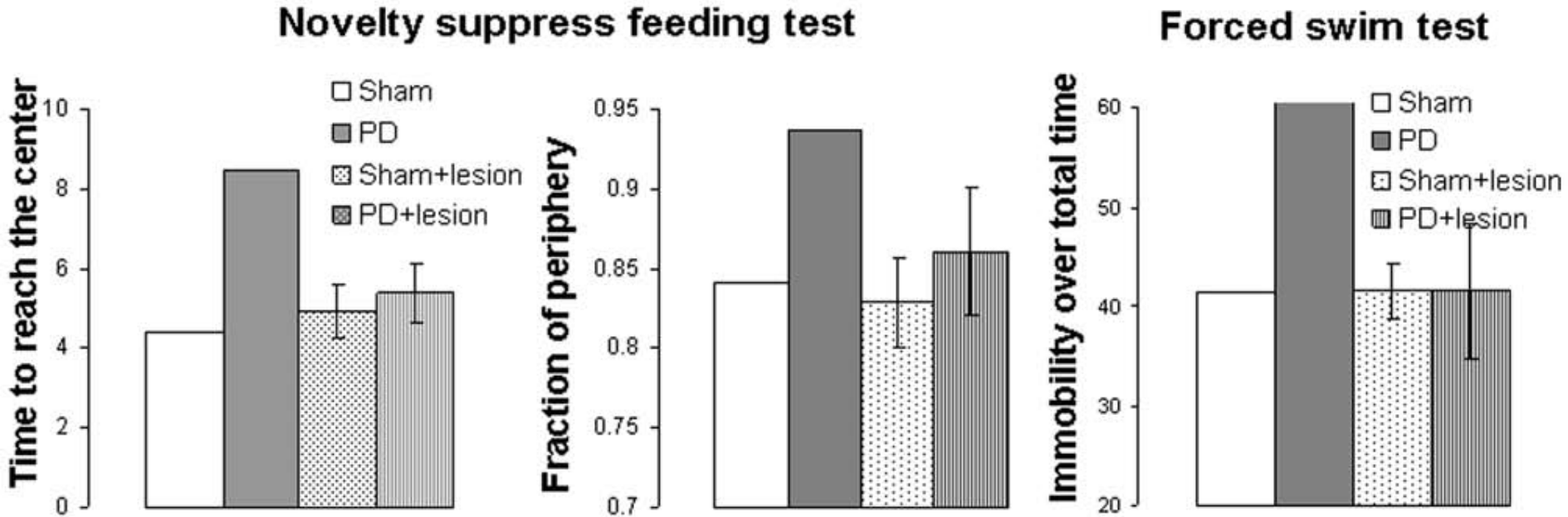
Novelty suppress feeding test
Time to reach the center
0
2
4
6
8
10
Sham
PD
Sham+lesion
PD+lesion
Fraction of periphery
0.7
0.75
0.8
0.85
0.9
0.95
Forced swim test
Immobility over total time
20
30
40
50
60
Sham
PD
Sham+lesion
PD+lesion